Frontiers in Bioscience Landmark

Front. Biosci. (Landmark Ed) **2022**; 27(12): 336
https://doi.org/10.31083/j.fbl2712336

Original Research

PYCR in Kidney Renal Papillary Cell Carcinoma: Expression, Prognosis, Gene Regulation Network, and Regulation Targets

Zheng Shao[1], Lingling Lu[1], Yongshi Cui[1], Li Deng[1], Qinying Xu[1], Quanyan Liang[1], Xiaoyong Lu[1], Juying Zhang[1], Jv Chen[2,*], Yongli Situ[1,*]

[1]Department of Parasitology, Guangdong Medical University, 524023 Zhanjiang, Guangdong, China
[2]Department of Pharmacy, Affiliated Hospital of Guangdong Medical University, 524001 Zhanjiang, Guangdong, China
*Correspondence: chenjv1990@126.com (Jv Chen); styl1987@126.com (Yongli Situ)
Academic Editor: Alfonso Urbanucci
Submitted: 2 September 2022 Revised: 17 November 2022 Accepted: 25 November 2022 Published: 28 December 2022

Abstract

Background: Pyrroline-5-carboxylate reductase (PYCR) includes three human genes encoding three isozymes, *PYCR1*, *PYCR2*, and *PYCR3* (or *PYCRL*), which facilitate the final step in the conversion of glutamine to proline. These genes play important roles in regulating the cell cycle and redox homeostasis as well as promoting growth signaling pathways. Proline is abnormally upregulated in a variety of cancers, and as the last key enzyme in proline production, PYCR plays an integral role in promoting tumorigenesis and cancer progression. However, its role in patients with kidney renal papillary cell carcinoma (KIRP) has not been fully elucidated. In this study, we aimed to systematically analyze the expression, gene regulatory network, prognostic value, and target prediction of PYCR in patients with KIRP, elucidate the association between PYCR expression and KIRP, and identify potential new targets for the clinical treatment of KIRP. **Methods**: We systematically analyzed the expression, prognosis, gene regulatory network, and regulatory targets of *PYCR1, PYCR2,* and *PYCRL* in KIRP using multiple online databases including cBioPortal, STRING, MethSurv, GeneMANIA, Gene Expression Profiling Interactive Analysis (GEPIA), Metascape, UALCAN, LinkedOmics, and TIMER. **Results**: The expression levels of *PYCR1*, *PYCR2,* and *PYCRL* were considerably upregulated in patients with KIRP based on sample type, sex, age, and individual cancer stage. *PYCR1* and *PYCR2* transcript levels were markedly upregulated in females than in males, and patients aged 21–40 years had higher *PYCR1* and *PYCR2* transcript levels than those in other age groups. Interestingly, *PYCR2* transcript levels gradually decreased with age. In addition, the expressions of *PYCR1* and *PYCR2* were notably correlated with the pathological stage of KIRP. Patients with KIRP with low *PYCR1* and *PYCR2* expression had longer survival than those with high *PYCR1* and *PYCR2* expression. *PYCR1*, *PYCR2,* and *PYCRL* were altered by 4%, 7%, and 6%, respectively, in 280 patients with KIRP. The methylation levels of cytosine-phosphate-guanine (CpG) sites in PYCR were markedly correlated with the prognosis of patients with KIRP. *PYCR1*, *PYCR2*, *PYCRL,* and their neighboring genes form a complex network of interactions. The molecular functions of the genes, as demonstrated by their corresponding Kyoto Encyclopedia of Genes and Genomes (KEGG) pathway analyses, included calcium channel activity, phospholipid binding, RNA polymerase II-specificity, and kinase and GTPase-regulatory activities. *PYCR1*, *PYCR2*, and *PYCRL* targeted miR-21, miR-221, and miR-222, resulting in a better prognosis of KIRP. We analyzed mRNA sequencing data from 290 patients with KIRP and found that *ADA*, *NPM3*, and *TKT* were positively associated with *PYCR1* expression; *PFDN2*, *JTB*, and *HAX1* were positively correlated with *PYCR2* expression; *SHARPIN*, *YDJC*, and *NUBP2* were positively correlated with *PYCRL* expression; *PYCR1* was positively correlated with B cell and CD8+ T-cell infiltration levels; macrophage infiltration was negatively correlated with *PYCR2* expression; and *PYCRL* expression was negatively correlated with B-cell, CD8+ T cell, and dendritic cell infiltration levels. **Conclusions**: *PYCR1*, *PYCR2,* and *PYCRL* may be potential therapeutic and prognostic biomarkers for patients with KIRP. The regulation of microRNAs (miRNAs), including miR-21, miR-221, and miR-222, may prove an important strategy for KIRP treatment.

Keywords: *PYCR1*; *PYCR2*; *PYCRL*; kidney renal papillary cell carcinoma; target prediction; gene regulation network

1. Introduction

Cancer is the leading cause of human death and a major public health problem in most countries [1,2]. Kidney renal papillary cell carcinoma (KIRP) accounts for 10–20% of renal cell carcinomas (RCC) and is the second most common type of RCC [3]. Currently, the efficacy of therapeutic drugs remains unsatisfactory in clinical practice [4]. The etiology of KIRP remains unclear. Some studies have reported that the loss or mutation of various oncogenes in patients with KIRP, which leads to the excitation or inhibition of their functions, is one of the inevitable initial steps in the occurrence and development of KIRP [5]. Therefore, mining new biomarkers and potential regulatory targets is crucial to improve the morbidity and survival of patients with KIRP.

Pyrroline-5-carboxylate reductase (PYCR) includes three human genes encoding three isozymes, *PYCR1*, *PYCR2*, and *PYCR3* (or *PYCRL*), which facilitate the final step in the conversion of glutamine to proline. PYCR is upregulated in various cancer tissues [6]. High expression

of PYCR is positively correlated with poor cancer prognosis. Increased expression of PYCR leads to elevated proline concentrations, which are thought to be metabolic addictions in cancer cells, making proline a trusted therapeutic target [7]. Numerous studies have shown that PYCR plays a crucial role in tumor growth and progression [8–10]. In addition, proline has been shown to act as a potent anti-oxidative stress agent capable of protecting tumor cells from various reactive oxygen species inducers. Taken together, downregulating the expression level of PYCR may be an effective cancer treatment strategy and is expected to be a target for blocking tumor progression and improving survival.

The role of PYCR in KIRP is not well understood. Therefore, this study systematically analyzed the expression, gene regulatory network, prognostic value, and target prediction of PYCR in patients with KIRP, elucidated the association between PYCR and KIRP, and identified new potential targets for KIRP therapy.

2. Materials and Methods

2.1 UALCAN

UALCAN (http://ualcan.path.uab.edu/analysis.html) is an online professional database for analyzing tumor gene expression and methylation levels [11–13]. We used UALCAN to analyze the expression and methylation levels of *PYCR1*, *PYCR2*, and *PYCRL* in healthy subjects and patients with KIRP. We used the student's *t*-test for comparative analysis, and the difference was considered significant at a *p*-value less than 0.05.

2.2 GEPIA

Gene Expression Profiling (GEPIA) (http://gepia.cancer-pku.cn/index.html) is a free online platform for analyzing the correlation of gene expression levels with tumor pathological stage and prognostic value [13]. We used GEPIA to analyze the pathological staging correlation and prognostic value of the expression level of *PYCR1*, *PYCR2*, and *PYCRL* in patients with KIRP. Student's *t*-test was used for comparative analysis, and differences were considered significant at a *p*-value less than 0.05.

2.3 cBioPortal

cBioPortal (http://cbioportal.org) is an online professional database used to analyze genetic alterations in tumors [11–13]. We used the cBioPortal database to analyze genetic alterations in *PYCR1*, *PYCR2*, *PYCRL*, and their neighboring genes. A total of 280 KIRP samples were analyzed, and mRNA expression z-scores were obtained relative to all samples (log RNA Seq V2 RSEM) using a z-score threshold of $\pm$ 2.0.

2.4 STRING

STRING (https://string-db.org/cgi/input.pl) is an online professional database that analyzes protein-protein interactions (PPI) [13]. We used STRING to build a low-confidence level (0.150) PPI network and screening criteria for species defined as "humans". Finally, K-means cluster analysis was performed on *PYCR1*, *PYCR2*, *PYCRL*, and their neighboring genes.

2.5 GeneMANIA

GeneMANIA (http://www.genemania.org) is a free professional tool used to analyze gene functions [13]. We used GeneMANIA to explore the functions of *PYCR1*, *PYCR2*, *PYCRL*, and their altered neighboring genes.

2.6 Metascape

Metascape (https://metascape.org) is a professional-free tool that analyzes Gene Ontology (GO) functions and the Kyoto Encyclopedia of Genes and Genomes (KEGG) pathway enrichment [13]. We used Metascape to analyze the GO function and KEGG pathway enrichment of *PYCR1*, *PYCR2*, *PYCRL*, and their altered neighboring genes in KIRP.

2.7 LinkedOmics

LinkedOmics (http://www.linkedomics.org/) is a free online platform used to analyze miRNA target enrichment and differentially expressed genes associated with tumor genes [13]. The LinkedOmics database was used to analyze miRNA target enrichment and differentially expressed genes associated with *PYCR1*, *PYCR2*, and *PYCRL*.

2.8 TIMER

TIMER (https://cistrome.shinyapps.io/timer/) is a specialized database that systematically analyzes tumor genes associated with infiltrating immune cells [11–13]. We used TIMER to analyze the correlation between *PYCR1*, *PYCR2*, and *PYCRL* expression and immune cell infiltration.

2.9 MethSurv

MethSurv (https://biit.cs.ut.ee/methsurv/) is a free online platform that provides survival analyses based on DNA methylation. We used MethSurv to analyze DNA methylation and prognosis at PYCR sites in patients with KIRP.

3. Results

3.1 PYCR Expression in Patients with KIRP

We first compared the expression levels of *PYCR1*, *PYCR2*, and *PYCRL* in patients with KIRP according to sample type, sex, age, and individual cancer stage. Our results showed that *PYCR1*, *PYCR2*, and *PYCRL* transcript levels were significantly upregulated in patients with KIRP ($p < 0.05$; Fig. 1). In patients with KIRP, *PYCR1* and *PYCR2* transcript levels were significantly upregulated in females compared with in males ($p < 0.01$; Fig. 1B,F), and patients aged 21–40 years had higher *PYCR1* and *PYCR2* transcript levels than patients in other age groups ($p < 0.05$; Fig. 1C,G). Interestingly, *PYCR2* transcript levels gradually

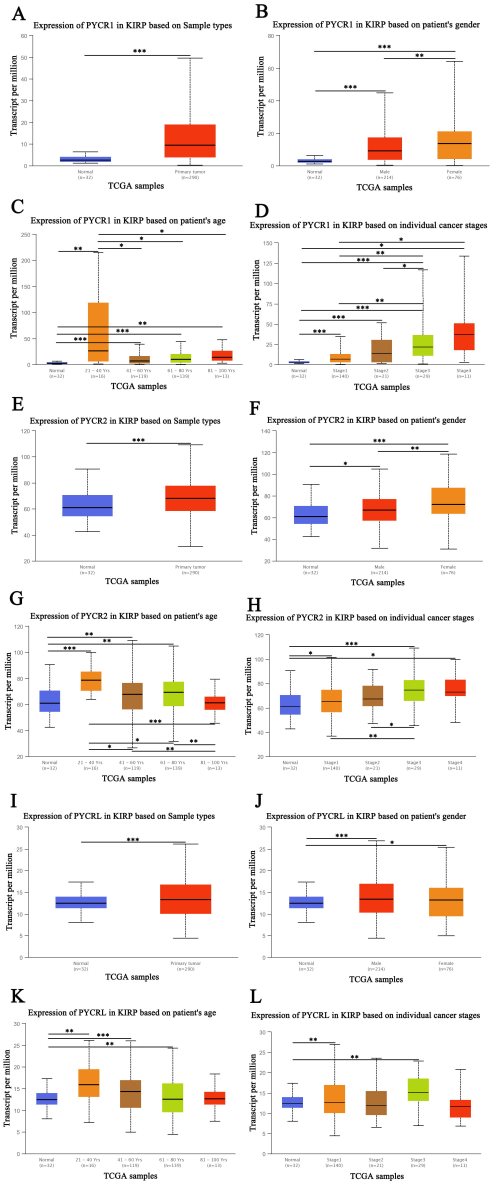

Fig. 1. The expression of PYCR in patients with KIRP (UALCAN). (A) The transcription expression of PYCR1 based on sample types. (B) The transcription expression of PYCR1 based on the sex of the patient. (C) The transcription expression of PYCR1 based on the age of the patient. (D) The transcription expression of PYCR1 based on individual cancer stage. (E) The transcription expression of PYCR2 based on sample types. (F) The transcription expression of PYCR2 based on the sex of the patient. (G) The transcription expression of PYCR2 based on the age of the patient. (H) The transcription expression of PYCR2 based on individual cancer stage. (I) The transcription expression of PYCRL based on sample types. (J) The transcription expression of PYCRL based on the sex of the patient. (K) The transcription expression of PYCRL based on the age of the patient. (L) The transcription expression of PYCRL based on individual cancer stage. *$p < 0.05$; **$p < 0.01$; ***$p < 0.001$.

decreased with age ($p < 0.05$; Fig. 1G). The transcript levels of *PYCR1* and *PYCR2* in different cancer stages were significantly higher than those in normal individuals and gradually increased with an increase in cancer stage ($p < 0.05$; Fig. 1D,H). In addition, we evaluated the correlation between the differential expression of *PYCR1* and *PYCR2* and the pathological stage of KIRP. We found a significant correlation between the expression of *PYCR1* ($p = 6.02 \times 10^{-14}$; Fig. 2A) and *PYCR2* ($p = 0.00145$; Fig. 2B) and the pathological stage of patients with KIRP. Finally, we used GEPIA to assess the prognostic value of *PYCR1*, *PYCR2*, and *PYCRL* expression in patients with KIRP. Our results showed that patients with KIRP with low *PYCR1* expression had a longer overall survival than those with high *PYCR1* expression ($p = 0.00094$; Fig. 3A). Similarly, patients with KIRP with low *PYCR1* and *PYCR2* expression had longer disease-free survival than those with high *PYCR1* and *PYCR2* expression ($p = 0.03$ and $p = 0.017$, respectively; Fig. 3B,D).

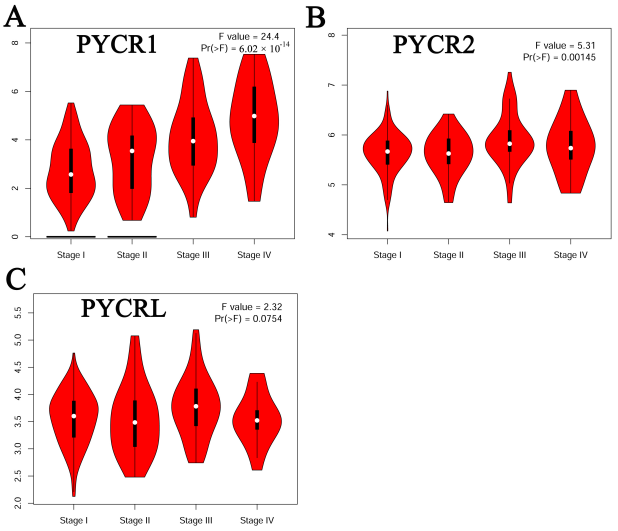

Fig. 2. Correlation between the pathological stage and different expressed PYCR of patients with KIRP (GEPIA). (A) *PYCR1*. (B) *PYCR2*. (C) *PYCRL*.

3.2 Genetic Alteration and Promoter Methylation of PYCR in Patients with KIRP

We further assessed the genetic alterations in *PYCR1*, *PYCR2*, and *PYCRL* in 280 patients with KIRP using TCGA. We found that *PYCR1* was altered by 4% in patients with KIRP, with the type of genetic alteration mainly including amplification, high RNA levels, and low RNA levels (Fig. 4A). However, *PYCR2* was altered by 7% in patients with KIRP, with the type of genetic alteration mainly including missense mutations, high RNA levels, and low RNA levels (Fig. 4B). *PYCRL* was altered by 6% in patients with KIRP, with the type of genetic alter-

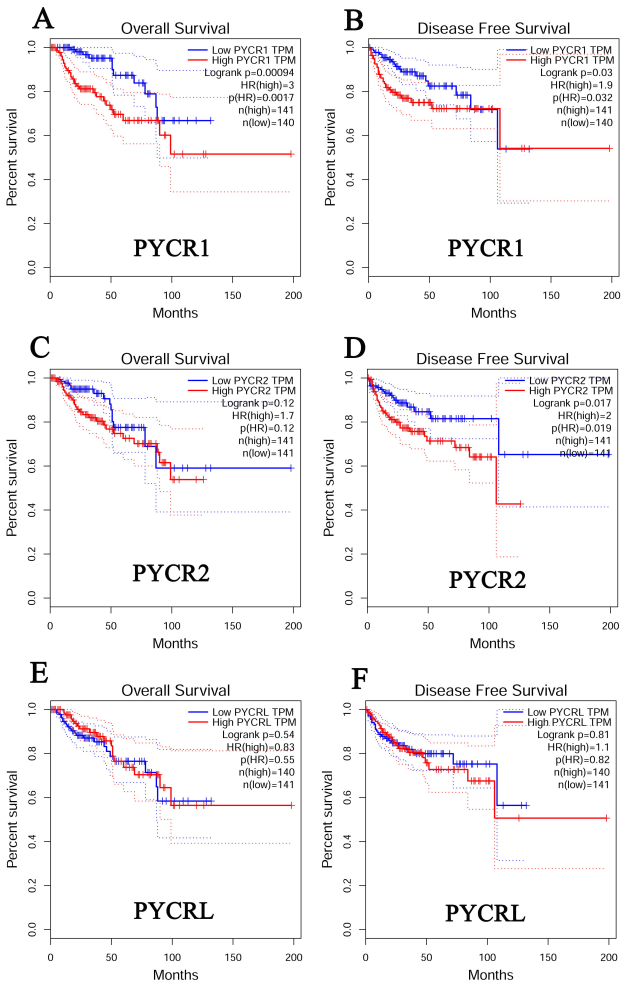

Fig. 3. The prognostic value of PYCR in KIRP (GEPIA). (A) The overall survival curve of *PYCR1* in patients with KIRP. (B) The disease-free survival cure of *PYCR1* in patients with KIRP. (C) The overall survival curve of *PYCR2* in patients with KIRP. (D) The disease-free survival cure of *PYCR2* in patients with KIRP. (E) The overall survival curve of *PYCRL*. (F) The disease-free survival cure of *PYCRL* in patients with KIRP.

ation mainly including missense mutations, truncating mutations, deep deletions, high RNA levels, and low RNA levels (Fig. 4C). Next, we assessed the promoter methylation levels of *PYCR1*, *PYCR2*, and *PYCRL* in patients with KIRP using UALCAN. We found that *PYCR1* and *PYCRL* promoter methylation levels were significantly downregulated in patients with KIRP ($p < 0.05$; Fig. 4D,F). Among the 18 predicted CpG sites of *PYCR1*, cg25759517 and cg19202384 were significantly correlated with KIRP prognosis (Fig. 5A) (Table 1). Patients with high *PYCR1* methylation at these CpG sites had better overall survival than those with low *PYCR1* methylation (Fig. 5B,C). Furthermore, Among the nine predicted CpG sites of *PYCR2*, cg07049680, cg23091741, and cg06086141 were considerably correlated with KIRP prognosis (Fig. 5D) (Table 1). Patients with high *PYCR2* methylation at CpG sites

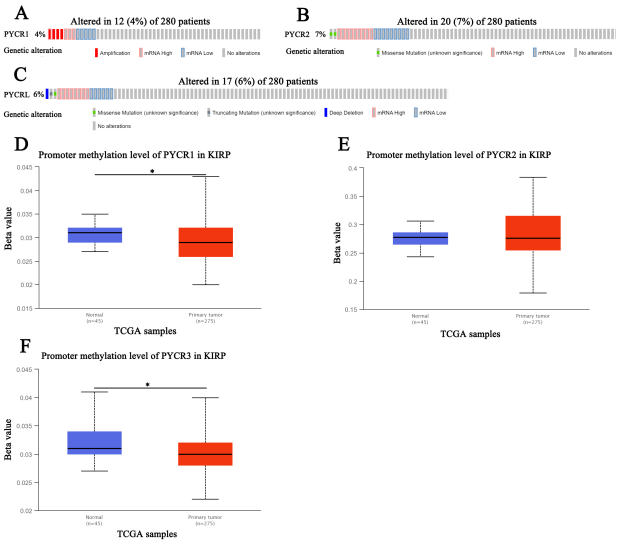

Fig. 4. Genetic alteration and promoter methylation of PYCR in KIRP (UALCAN). (A) Genetic alteration of *PYCR1*in patients with KIRP. (B) Genetic alteration of *PYCR2* in patients with KIRP. (C) Genetic alteration of *PYCRL* in patients with KIRP. (D) Promoter methylation of *PYCR1*in healthy individuals and patients with KIRP. (E) Promoter methylation of *PYCR2* in healthy individuals and patients with KIRP. (F) Promoter methylation of *PYCRL* in healthy individuals and patients with KIRP.

(cg07049680 and cg23091741) had worse overall survival than patients with low *PYCR2* methylation (Fig. 5E,F). However, patients with high *PYCR2* methylation at CpG sites (cg06086141) had better overall survival than patients with low *PYCR2* methylation (Fig. 5G). Among the 12 predicted CpG sites of *PYCRL*, cg26507094 was markedly correlated with KIRP prognosis (Fig. 5H) (Table 1). Patients with high *PYCRL* methylation at these CpG sites had worse overall survival than those with low *PYCRL* methylation (Fig. 5I).

3.3 Neighboring Gene Alteration and PYCR Interaction Network in Patients with KIRP

We evaluated alterations in the neighboring genes of *PYCR1*, *PYCR2*, and *PYCRL* in patients with KIRP using cBioPortal. We found a gene alteration frequency of ≥25.00%, ≥10.00%, and ≥11.76% for the 50 most frequently altered neighboring genes of *PYCR1*, *PYCR2*, and *PYCRL* in patients with KIRP, respectively (Tables 2,3,4). The most frequently altered neighboring genes of *PYCR1* in patients with KIRP were *ALYREF* (33.33%), *ANAPC11* (33.33%), and *ARHGDIA* (33.33%) (Table 2). However, *PBRM1* (20.00%), *CDKN2A* (20.00%), and *ALK* (15.00%) were the most frequently altered neighboring genes of *PYCR2* in patients with KIRP (Table 3). The most frequently altered neighboring genes of *PYCRL* in patients with KIRP were *MT-CO2* (23.53%), *BLK* (17.65%), and *C2CD5* (17.65%) (Table 4).

Table 1. The significant prognostic values of CpG in PYCR (MethSurv).

Gene symbol	CpG name	Hazard Ratio	Confidence interval (CI)	Likelihood ratio (LR) test *p* value	University of California Santa Cruz (UCSC) Ref gene group	Relation to UCSC CpG Island
PYCR1	cg25759517	0.512	(0.27; 0.971)	0.038	TSS200	Island
	cg19202384	0.452	(0.235; 0.871)	0.015	Body	N_Shore
PYCR2	cg07049680	1.907	(1.003; 3.626)	0.045	TSS1500	Island
	cg23091741	2.265	(1.151; 4.458)	0.014	Body	Island
	cg06086141	0.422	(0.21; 0.847)	0.011	TSS1500	S_Shore
PYCRL	cg26507094	2.611	(1.342; 5.079)	0.0033	Body	Island

We further evaluated the potential interactions between *PYCR1*, *PYCR2*, *PYCRL*, and their neighboring genes. Our results showed that 43 nodes, 188 edges, and 3 clusters were obtained in the constructed PPI network of *PYCR1* and its neighboring genes in patients with KIRP (Fig. 6A). Furthermore, *PYCR1* and its neighboring genes were linked to a complex interaction network (70 genes and 226 edges) through co-expression, physical interactions, shared protein domains, and prediction (Fig. 6B). However, we found that 46 nodes, 158 edges, and 3 clusters were obtained in the constructed PPI network of *PYCR2* and its neighboring genes in patients with KIRP (Fig. 6C). Furthermore, *PYCR2* and its neighboring genes were linked to a complex interaction network (71 genes and 217 edges) through co-expression, physical interactions, genetic interactions, and prediction (Fig. 6D). Additionally, 33 nodes, 126 edges, and 3 clusters were obtained in the constructed PPI network of *PYCRL* and its neighboring genes in patients with KIRP (Fig. 6E). In addition, *PYCRL* and its neighboring genes were linked to a complex interaction network (60 genes and 188 edges) through co-expression, physical interactions, shared protein domains, and prediction (Fig. 6F).

3.4 GO and KEGG Pathway Enrichment Analyses

We further performed GO and KEGG pathway enrichment analyses of *PYCR1*, *PYCR2*, *PYCRL*, and their top 50 altered neighboring genes in patients with KIRP using Metascape. We found that the molecular functions related to *PYCR1* and its neighboring genes mainly included voltage-gated calcium channel activity, phospholipid binding, and ubiquitin-like protein ligase binding (Fig. 7A). Their cellular components include nuclear ubiquitin ligase complexes, tertiary granules, and cation channel complexes (Fig. 7B). Their biological processes included protein localization to lysosomes, regulation of wound healing, and negative regulation of cell activation (Fig. 7C). Arrhythmogenic right ventricular cardiomyopathy and cardiac muscle contraction were enriched according to KEGG pathway analysis (Fig. 7D). However, our results showed that nuclear receptor binding, DNA-binding transcription activator activity, RNA polymerase II-specific, phosphotransferase activity, alcohol group as acceptor, and oxidoreductase activity were molecular functions related to *PYCR2* and its neighboring genes (Fig. 7E). The RNA polymerase II transcription regulator complex and the cytoplasmic region were their cellular components (Fig. 7F). Cellular response to oxidative stress, regulation of the G1/S transition of the mitotic cell cycle, and the enzyme-linked receptor protein signaling pathway were the main biological processes (Fig. 7G). KEGG pathway analysis revealed that *PYCR2* and its neighboring genes were associated with pathways in cancer (Fig. 7H). Furthermore, the molecular functions related to *PYCRL* and its neighboring genes mainly include oxidoreductase activity, kinase activity, and GTPase regulator activity (Fig. 7I). The cellular components were spindles (Fig. 7J). The mitotic cell cycle process, positive regulation of protein localization, small molecule biosynthetic process, and chemotaxis were the main biological processes (Fig. 7K). Arginine and proline metabolism and amino acid biosynthesis were found to be enriched according to KEGG pathway analysis (Fig. 7L).

3.5 miRNA Targets of PYCR in Patients with KIRP

We analyzed the miRNA targets of *PYCR1*, *PYCR2*, and *PYCRL* using LinkedOmics. ATAAGCT (miR-21), ATGTAGC (miR-221 and miR-222), GTTATAT (miR-410), ATAGGAA (miR-202), and TACAATC (miR-508) were the top five miRNA targets of *PYCR1* in patients with KIRP (False discovery rate (FDP) <0.05; Table 5). The top five miRNA targets of *PYCR2* in patients with KIRP were TGCACTG (miR-148A, miR-152, and miR-148B); CTATGCA (miR-153); AATGTGA (miR-23A and miR-23B); ATGTAGC (miR-221 and miR-222); and TGCTGCT (miR-15A, miR-16, miR-15B, miR-195, miR-424, and miR-497) (FDP = 0; Table 6). Besides, AAGCCAT (miR-135A and miR-135B), AAAGGGA (miR-204 and miR-211), TCTGATC (miR-383), AGCACTT (miR-93, miR-302A, miR-302B, miR-302C, miR-302D, miR-372, miR-373, miR-520E, miR-520A, miR-526B, miR-520B, miR-520C, and miR-520D), and ACACTGG (miR-199A and miR-199B) were the top five miRNA targets of *PYCRL* in patients with KIRP (FDP = 0; Table 7).

3.6 Correlation of Differentially Expressed Genes and PYCR Expression in Patients with KIRP

We analyzed mRNA sequencing data from 290 patients with KIRP using the LinkedOmics TCGA database. Our results showed that the expression of 20,023 genes

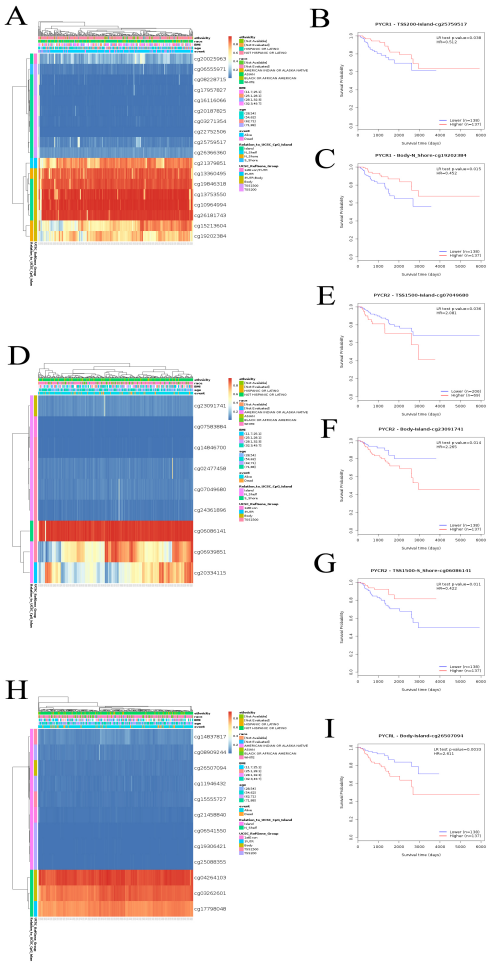

Fig. 5. DNA methylation at CpG sites and prognostic value of PYCR in KIRP (MethSurv). (A) Heatmap showing the *PYCR1* DNA methylation at CpG sites. (B) Patients with KIRP with higher *PYCR1* methylation of cg25759517 CpG sites had a better overall survival than those with lower *PYCR1* methylation (HR = 0.512, p = 0.038). (C) Patients with KIRP with higher *PYCR1* methylation of cg19202384 CpG sites had a better overall survival than those with lower *PYCR1* methylation (HR = 0.452, p = 0.015). (D) Heatmap showing the *PYCR2* DNA methylation at CpG sites. (E) Patients with KIRP with higher *PYCR2* methylation of cg07049680 CpG sites had a worse overall survival than those with lower *PYCR2* methylation (HR = 1.907, p = 0.045). (F) Patients with KIRP with higher *PYCR2* methylation of cg23091741 CpG sites had a worse overall survival than those with lower *PYCR2* methylation (HR = 2.265, p = 0.014). (G) Patients with KIRP with higher *PYCR2* methylation of cg23091741 CpG sites had a better overall survival than those with lower *PYCR1* methylation (HR = 0.422, p = 0.011). (H) Heatmap showing the *PYCRL* DNA methylation at CpG sites. (I) Patients with KIRP with higher *PYCRL* methylation of cg26507094 CpG sites had a worse overall survival than those with lower *PYCRL* methylation (HR = 2.611, p = 0.0033).

Table 2. The top 50 of *PYCR1* neighbor gene alterations in KIRP (cBioPortal).

Gene	Altered group	Unaltered group	p-value
ALYREF	4 (33.33%)	0 (0.00%)	1.98×10^{-6}
ANAPC11	4 (33.33%)	0 (0.00%)	1.98×10^{-6}
ARHGDIA	4 (33.33%)	0 (0.00%)	1.98×10^{-6}
ARL16	4 (33.33%)	0 (0.00%)	1.98×10^{-6}
CCDC137	4 (33.33%)	0 (0.00%)	1.98×10^{-6}
GCGR	4 (33.33%)	0 (0.00%)	1.98×10^{-6}
MAFG	4 (33.33%)	0 (0.00%)	1.98×10^{-6}
MCRIP1	4 (33.33%)	0 (0.00%)	1.98×10^{-6}
MRPL12	4 (33.33%)	0 (0.00%)	1.98×10^{-6}
MYADML2	4 (33.33%)	0 (0.00%)	1.98×10^{-6}
NPB	4 (33.33%)	0 (0.00%)	1.98×10^{-6}
P4HB	4 (33.33%)	0 (0.00%)	1.98×10^{-6}
PPP1R27	4 (33.33%)	0 (0.00%)	1.98×10^{-6}
SLC25A10	4 (33.33%)	0 (0.00%)	1.98×10^{-6}
SLC26A11	4 (33.33%)	0 (0.00%)	1.98×10^{-6}
WDR45B	4 (33.33%)	0 (0.00%)	1.98×10^{-6}
AXIN2	4 (33.33%)	1 (0.37%)	9.65×10^{-6}
HGS	4 (33.33%)	1 (0.37%)	9.65×10^{-6}
RNF43	4 (33.33%)	1 (0.37%)	9.65×10^{-6}
TMC6	4 (33.33%)	1 (0.37%)	9.65×10^{-6}
PCYT2	4 (33.33%)	2 (0.75%)	2.83×10^{-5}
TBC1D16	4 (33.33%)	2 (0.75%)	2.83×10^{-5}
TRIM37	4 (33.33%)	2 (0.75%)	2.83×10^{-5}
AANAT	3 (25.00%)	0 (0.00%)	6.08×10^{-5}
ABCA9	3 (25.00%)	0 (0.00%)	6.08×10^{-5}
ACTG1	3 (25.00%)	0 (0.00%)	6.08×10^{-5}
AFMID	3 (25.00%)	0 (0.00%)	6.08×10^{-5}
AMZ2P1	3 (25.00%)	0 (0.00%)	6.08×10^{-5}
APOH	3 (25.00%)	0 (0.00%)	6.08×10^{-5}
ARMC7	3 (25.00%)	0 (0.00%)	6.08×10^{-5}
ARSG	3 (25.00%)	0 (0.00%)	6.08×10^{-5}
ASPSCR1	3 (25.00%)	0 (0.00%)	6.08×10^{-5}
B3GNTL1	3 (25.00%)	0 (0.00%)	6.08×10^{-5}
BTBD17	3 (25.00%)	0 (0.00%)	6.08×10^{-5}
C17ORF58	3 (25.00%)	0 (0.00%)	6.08×10^{-5}
C17ORF99	3 (25.00%)	0 (0.00%)	6.08×10^{-5}
C1QTNF1	3 (25.00%)	0 (0.00%)	6.08×10^{-5}
CACNG1	3 (25.00%)	0 (0.00%)	6.08×10^{-5}
CACNG4	3 (25.00%)	0 (0.00%)	6.08×10^{-5}
CACNG5	3 (25.00%)	0 (0.00%)	6.08×10^{-5}
CANT1	3 (25.00%)	0 (0.00%)	6.08×10^{-5}
CASKIN2	3 (25.00%)	0 (0.00%)	6.08×10^{-5}
CBX2	3 (25.00%)	0 (0.00%)	6.08×10^{-5}
CBX8	3 (25.00%)	0 (0.00%)	6.08×10^{-5}
CD300A	3 (25.00%)	0 (0.00%)	6.08×10^{-5}
CD300C	3 (25.00%)	0 (0.00%)	6.08×10^{-5}
CD300E	3 (25.00%)	0 (0.00%)	6.08×10^{-5}
CD300LB	3 (25.00%)	0 (0.00%)	6.08×10^{-5}
CD300LD	3 (25.00%)	0 (0.00%)	6.08×10^{-5}
CD300LF	3 (25.00%)	0 (0.00%)	6.08×10^{-5}

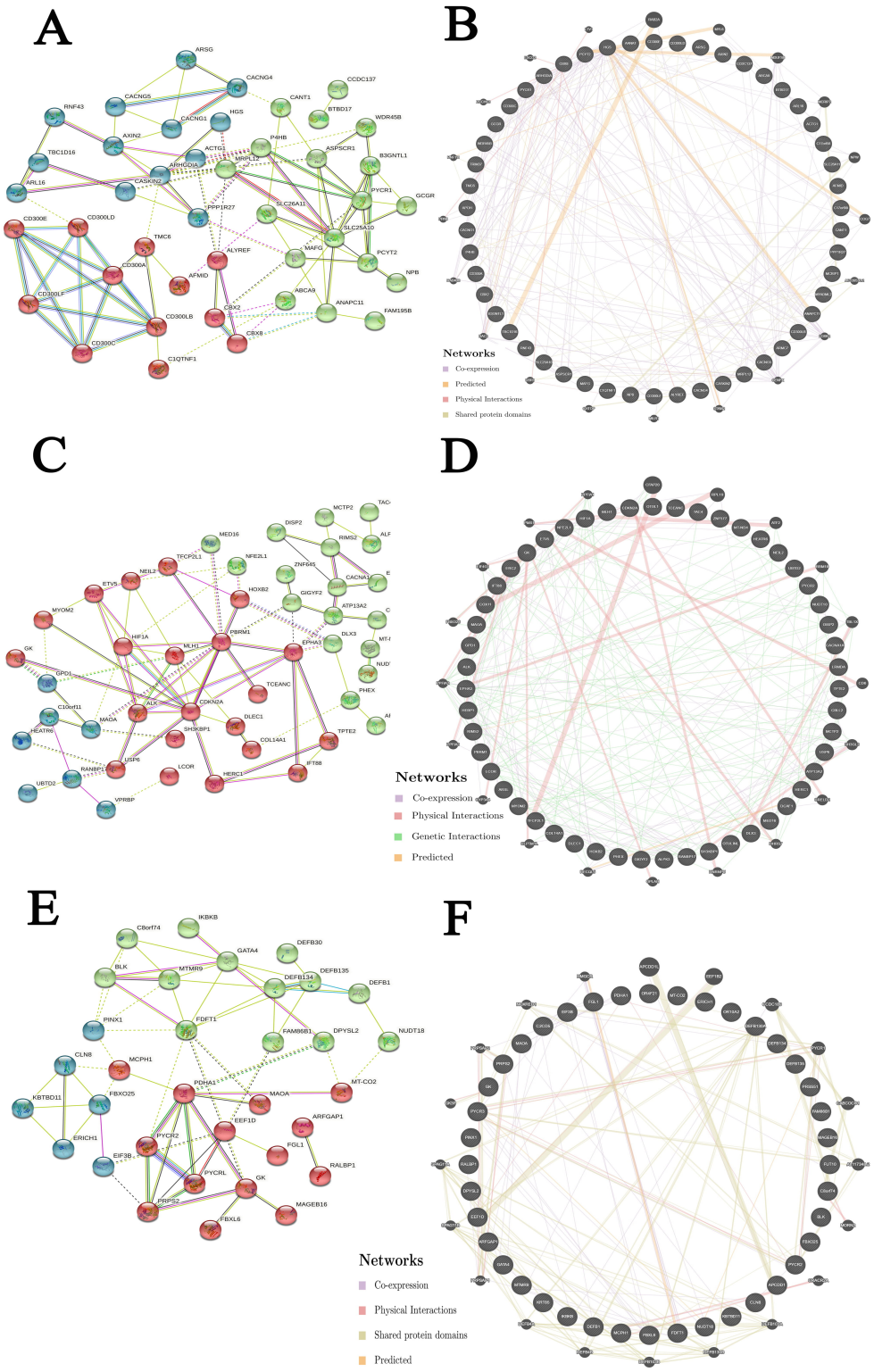

Fig. 6. Interaction analyses of PYCR and their neighboring genes in KIRP (STRING and GeneMANIA). (A) PPI network of *PYCR1* and its neighboring genes in patients with KIRP (STRING). (B) Network analyses of *PYCR1* and its neighboring genes in patients with KIRP (GeneMANIA). (C) PPI network of *PYCR2* and its neighboring genes in patients with KIRP (STRING). (D) Network analyses of *PYCR2* and its neighboring genes in patients with KIRP (GeneMANIA). (E) PPI network of *PYCRL* and its neighboring genes in patients with KIRP (STRING). (F) Network analyses of *PYCRL* and its neighboring genes in patients with KIRP (GeneMANIA).

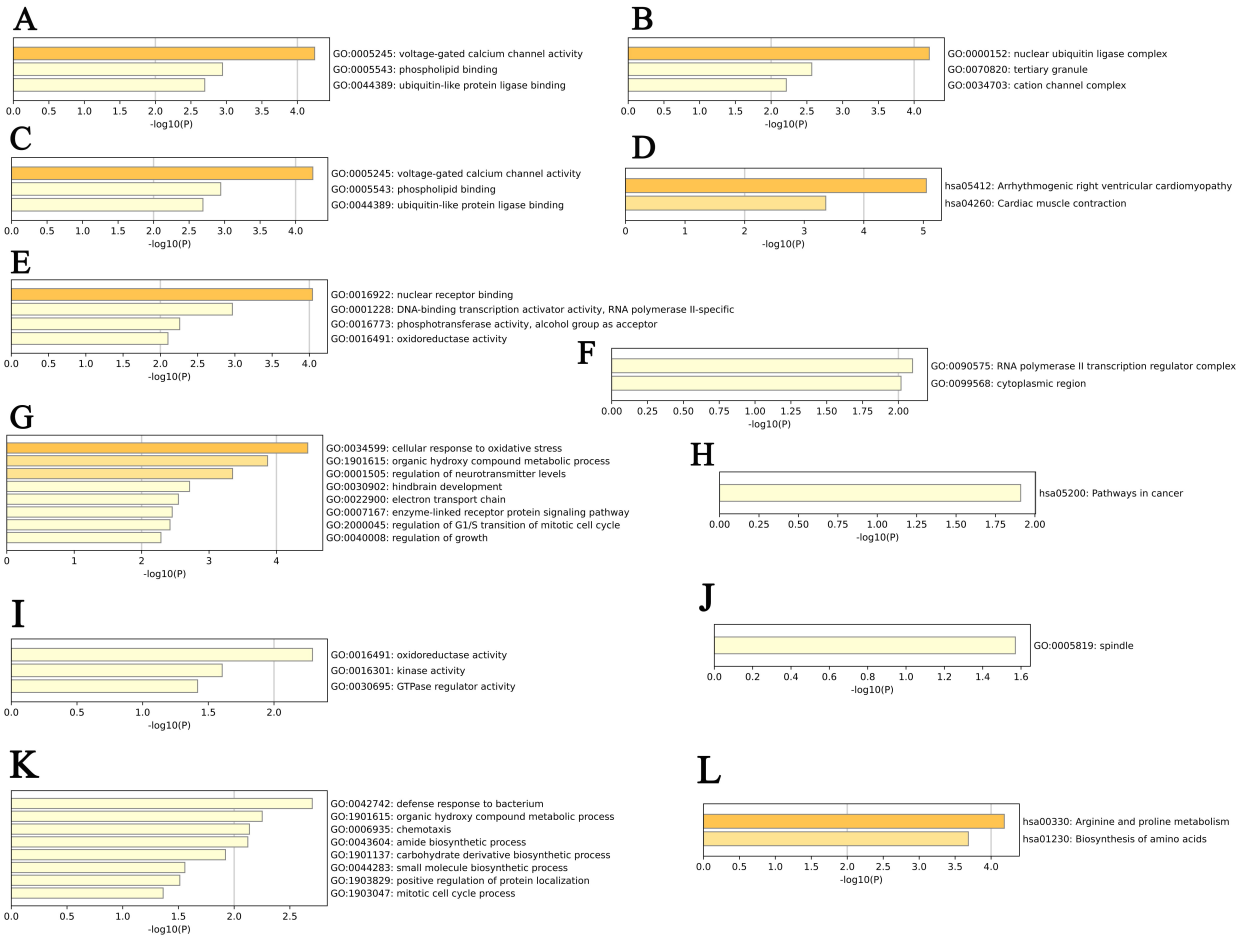

Fig. 7. GO function and KEGG pathways enrichment analyses of *PYCR1*, *PYCR2*, *PYCRL*, and their neighboring genes in patients with KIRP (Metascape). (A) Molecular functions of *PYCR1* and its neighboring genes. (B) Cellular components of *PYCR1* and its neighboring genes. (C) Biological processes of *PYCR1* and its neighboring genes. (D) KEGG pathway analysis of *PYCR1* and its neighboring genes. (E) Molecular functions of *PYCR2* and its neighboring genes. (F) Cellular components of *PYCR2* and its neighboring genes. (G) Biological processes of *PYCR2* and its neighboring genes. (H) KEGG pathway analysis of *PYCR2* and its neighboring genes. (I) Molecular functions of *PYCRL* and its neighboring genes. (J) Cellular components of *PYCRL* and its neighboring genes. (K) Biological processes of *PYCRL* and its neighboring genes. (L) KEGG pathway analysis of *PYCRL* and its neighboring genes.

correlated with *PYCR1* expression, of which, 10,041 and 9982 genes were positively and negatively correlated with *PYCR1* expression, respectively (Fig. 8A). Furthermore, we screened 50 genes significantly positively and negatively correlated with *PYCR1* expression in patients with KIRP ($p < 0.05$; Fig. 8B,C). *ADA* (Pearson correlation coefficient = 0.6049, $p = 2.509 \times 10^{-30}$; Fig. 8D), *NPM3* (Pearson correlation coefficient = 0.5955, $p = 3.231 \times 10^{-29}$; Fig. 8E), and *TKT* (Pearson correlation coefficient = 0.5906, $p = 1.188 \times 10^{-28}$; Fig. 8F) were the top three genes with expressions positively correlated with the *PYCR1* expression. However, we found that 20,023 genes were correlated with *PYCR2* expression, of which, 10,750 and 9273 genes were positively and negatively correlated with *PYCR2* expression, respectively (Fig. 8G). In addition, we screened 50 genes significantly positively and negatively correlated with *PYCR2* expression in patients with KIRP ($p < 0.05$; Fig. 8H,I). Among these, *PFDN2* (Pearson correlation coefficient = 0.6955, $p = 3.059 \times 10^{-43}$; Fig. 8J), *JTB* (Pearson correlation coefficient = 0.6863, $p = 1.017 \times 10^{-41}$; Fig. 8K), and *HAX1* (Pearson correlation coefficient = 0.3837, $p = 2.663 \times 10^{-41}$; Fig. 8L) were the top three genes positively correlated with *PYCR2* expression. Furthermore, 9195 and 10,828 genes were positively and negatively correlated with *PYCRL* expression, respectively (Fig. 8M). In addition, we screened 50 genes significantly positively and negatively correlated with *PYCRL* expression in patients with KIRP ($p < 0.05$; Fig. 8N,O). Among which, *SHARPIN* (Pearson correlation coefficient = 0.7299, $p = 1.682 \times 10^{-49}$; Fig. 8P), *YDJC* (Pearson correlation coefficient = 0.7289, $p = 2.646 \times 10^{-49}$; Fig. 8Q), and *NUBP2* (Pearson correlation coefficient = 0.7249, $p = 1.585 \times 10^{-48}$; Fig. 8R) were the top three genes positively correlated with *PYCRL* expression.

Table 3. The top 50 of *PYCR2* neighbor gene alterations in KIRP (cBioPortal).

Gene	Altered group	Unaltered group	*p*-value
CBLL2	2 (10.00%)	0 (0.00%)	4.86×10^{-3}
DCAF1	2 (10.00%)	0 (0.00%)	4.86×10^{-3}
GK	2 (10.00%)	0 (0.00%)	4.86×10^{-3}
GPD1	2 (10.00%)	0 (0.00%)	4.86×10^{-3}
HIF1A	2 (10.00%)	0 (0.00%)	4.86×10^{-3}
IFT88	2 (10.00%)	0 (0.00%)	4.86×10^{-3}
MAOA	2 (10.00%)	0 (0.00%)	4.86×10^{-3}
OTOL1	2 (10.00%)	0 (0.00%)	4.86×10^{-3}
PHEX	2 (10.00%)	0 (0.00%)	4.86×10^{-3}
SH3KBP1	2 (10.00%)	0 (0.00%)	4.86×10^{-3}
TCEANC	2 (10.00%)	0 (0.00%)	4.86×10^{-3}
TFCP2L1	2 (10.00%)	0 (0.00%)	4.86×10^{-3}
TPTE2	2 (10.00%)	0 (0.00%)	4.86×10^{-3}
PBRM1	4 (20.00%)	8 (3.08%)	6.54×10^{-3}
ALK	3 (15.00%)	5 (1.92%)	0.0139
MYOM2	3 (15.00%)	5 (1.92%)	0.0139
ALPK3	2 (10.00%)	1 (0.38%)	0.014
COL14A1	2 (10.00%)	1 (0.38%)	0.014
ETV5	2 (10.00%)	1 (0.38%)	0.014
HEBP1	2 (10.00%)	1 (0.38%)	0.014
HOXB2	2 (10.00%)	1 (0.38%)	0.014
LRMDA	2 (10.00%)	1 (0.38%)	0.014
MCTP2	2 (10.00%)	1 (0.38%)	0.014
MED16	2 (10.00%)	1 (0.38%)	0.014
MLH1	2 (10.00%)	1 (0.38%)	0.014
NEIL2	2 (10.00%)	1 (0.38%)	0.014
NFE2L1	2 (10.00%)	1 (0.38%)	0.014
NUDT10	2 (10.00%)	1 (0.38%)	0.014
RIMS2	2 (10.00%)	1 (0.38%)	0.014
USP6	2 (10.00%)	1 (0.38%)	0.014
ZNF577	2 (10.00%)	1 (0.38%)	0.014
CDKN2A	4 (20.00%)	11 (4.23%)	0.0156
MT-ND4	4 (20.00%)	11 (4.23%)	0.0156
HERC1	3 (15.00%)	6 (2.31%)	0.0199
ARSL	2 (10.00%)	2 (0.77%)	0.0267
DISP2	2 (10.00%)	2 (0.77%)	0.0267
DLEC1	2 (10.00%)	2 (0.77%)	0.0267
DLX3	2 (10.00%)	2 (0.77%)	0.0267
ERC2	2 (10.00%)	2 (0.77%)	0.0267
LCOR	2 (10.00%)	2 (0.77%)	0.0267
OTULINL	2 (10.00%)	2 (0.77%)	0.0267
TAC4	2 (10.00%)	2 (0.77%)	0.0267
UBTD2	2 (10.00%)	2 (0.77%)	0.0267
GIGYF2	3 (15.00%)	7 (2.69%)	0.0272
ATP13A2	2 (10.00%)	3 (1.15%)	0.0426
CACNA1A	2 (10.00%)	3 (1.15%)	0.0426
COX11	2 (10.00%)	3 (1.15%)	0.0426
EPHA3	2 (10.00%)	3 (1.15%)	0.0426
HEATR6	2 (10.00%)	3 (1.15%)	0.0426
RANBP17	2 (10.00%)	3 (1.15%)	0.0426

Table 4. The top 50 of *PYCRL* neighbor gene alterations in KIRP (cBioPortal).

Gene	Altered group	Unaltered group	*p*-value
MT-CO2	4 (23.53%)	2 (0.76%)	1.32×10^{-4}
BLK	3 (17.65%)	1 (0.38%)	7.23×10^{-4}
C2CD5	3 (17.65%)	1 (0.38%)	7.23×10^{-4}
MCPH1	3 (17.65%)	2 (0.76%)	1.74×10^{-3}
APCDD1	2 (11.76%)	0 (0.00%)	3.48×10^{-3}
ARFGAP1	2 (11.76%)	0 (0.00%)	3.48×10^{-3}
C8ORF74	2 (11.76%)	0 (0.00%)	3.48×10^{-3}
CLN8	2 (11.76%)	0 (0.00%)	3.48×10^{-3}
DEFB1	2 (11.76%)	0 (0.00%)	3.48×10^{-3}
DEFB130A	2 (11.76%)	0 (0.00%)	3.48×10^{-3}
DEFB134	2 (11.76%)	0 (0.00%)	3.48×10^{-3}
DEFB135	2 (11.76%)	0 (0.00%)	3.48×10^{-3}
DPYSL2	2 (11.76%)	0 (0.00%)	3.48×10^{-3}
EEF1D	2 (11.76%)	0 (0.00%)	3.48×10^{-3}
EIF3B	2 (11.76%)	0 (0.00%)	3.48×10^{-3}
ERICH1	2 (11.76%)	0 (0.00%)	3.48×10^{-3}
FAM66A	2 (11.76%)	0 (0.00%)	3.48×10^{-3}
FAM66D	2 (11.76%)	0 (0.00%)	3.48×10^{-3}
FAM86B1	2 (11.76%)	0 (0.00%)	3.48×10^{-3}
FBXL6	2 (11.76%)	0 (0.00%)	3.48×10^{-3}
FBXO25	2 (11.76%)	0 (0.00%)	3.48×10^{-3}
FDFT1	2 (11.76%)	0 (0.00%)	3.48×10^{-3}
FGL1	2 (11.76%)	0 (0.00%)	3.48×10^{-3}
FUT10	2 (11.76%)	0 (0.00%)	3.48×10^{-3}
GATA4	2 (11.76%)	0 (0.00%)	3.48×10^{-3}
GK	2 (11.76%)	0 (0.00%)	3.48×10^{-3}
IKBKB	2 (11.76%)	0 (0.00%)	3.48×10^{-3}
KBTBD11	2 (11.76%)	0 (0.00%)	3.48×10^{-3}
KRT85	2 (11.76%)	0 (0.00%)	3.48×10^{-3}
LINC00208	2 (11.76%)	0 (0.00%)	3.48×10^{-3}
LINC00529	2 (11.76%)	0 (0.00%)	3.48×10^{-3}
LINC02905	2 (11.76%)	0 (0.00%)	3.48×10^{-3}
MAGEB16	2 (11.76%)	0 (0.00%)	3.48×10^{-3}
MAOA	2 (11.76%)	0 (0.00%)	3.48×10^{-3}
MIR124-1HG	2 (11.76%)	0 (0.00%)	3.48×10^{-3}
MTMR9	2 (11.76%)	0 (0.00%)	3.48×10^{-3}
NUDT18	2 (11.76%)	0 (0.00%)	3.48×10^{-3}
OR10A2	2 (11.76%)	0 (0.00%)	3.48×10^{-3}
OR4F21	2 (11.76%)	0 (0.00%)	3.48×10^{-3}
PDHA1	2 (11.76%)	0 (0.00%)	3.48×10^{-3}
PINX1	2 (11.76%)	0 (0.00%)	3.48×10^{-3}
PRPS2	2 (11.76%)	0 (0.00%)	3.48×10^{-3}
PRSS51	2 (11.76%)	0 (0.00%)	3.48×10^{-3}
PYCR2	2 (11.76%)	0 (0.00%)	3.48×10^{-3}
RALBP1	2 (11.76%)	0 (0.00%)	3.48×10^{-3}
RN7SKP159	2 (11.76%)	0 (0.00%)	3.48×10^{-3}
RN7SL293P	2 (11.76%)	0 (0.00%)	3.48×10^{-3}
RN7SL318P	2 (11.76%)	0 (0.00%)	3.48×10^{-3}
RNA5SP251	2 (11.76%)	0 (0.00%)	3.48×10^{-3}
RNA5SP252	2 (11.76%)	0 (0.00%)	3.48×10^{-3}

Table 5. The top five miRNA target of *PYCR1* in KIRP (LinkedOmics).

Gene set	Leading edge number	*p*-value	FDR
ATAAGCT, miR-21	40	0	0.012789
ATGTAGC, miR-221, miR-222	55	0	0.017763
GTTATAT, miR-410	32	0	0.018331
ATAGGAA, miR-202	35	0	0.018758
TACAATC, miR-508	26	0	0.018879

Table 6. The top five miRNA target of *PYCR2* in KIRP (LinkedOmics).

Gene set	Leading edge number	*p*-value	FDR
TGCACTG, miR-148A, miR-152, miR-148B	108	0	0
CTATGCA, miR-153	74	0	0
AATGTGA, miR-23A, miR-23B	126	0	0
ATGTAGC, miR-221, miR-222	50	0	0
TGCTGCT, miR-15A, miR-16, miR-15B, miR-195, miR-424, miR-497	207	0	0

Table 7. The top five miRNA target of *PYCRL* in KIRP (LinkedOmics).

Gene set	Leading edge number	*p*-value	FDR
AAGCCAT, miR-135A, miR-135B	140	0	0
AAAGGGA, miR-204, miR-211	77	0	0
TCTGATC, miR-383	18	0	0
AGCACTT, miR-93, miR-302A, miR-302B, miR-302C, miR-302D, miR-372, miR-373, miR-520E, miR-520A, miR-526B, miR-520B, miR-520C, miR-520D	145	0	0
ACACTGG, miR-199A, miR-199B	60	0	0

3.7 Immune Cell Infiltration and PYCR Expression in Patients with KIRP

We used TIMER to evaluate the relationship between immune cell infiltration and *PYCR1*, *PYCR2*, and *PYCRL* expression in patients with KIRP. Our results showed that the expression level of *PYCR1* in patients with KIRP was positively correlated with B cell (Cor = 0.217, $p = 4.71 \times 10^{-4}$) and CD8+ T cell (Cor = 0.219, $p = 3.99 \times 10^{-4}$) infiltration levels (Fig. 9A). However, we found that macrophage infiltration levels were negatively correlated with the expression level of *PYCR2* in patients with KIRP (Cor = –0.148, $p = 1.94 \times 10^{-2}$; Fig. 9B). The expression level of *PYCRL* in patients with KIRP was negatively correlated with B-cell (Cor = –0.198, $p = 1.43 \times 10^{-3}$), CD8+ T cell (Cor = –0.338, $p = 2.70 \times 10^{-8}$), and dendritic cell (Cor = –0.187, $p = 2.67 \times 10^{-3}$) infiltration levels (Fig. 9C). The expression level of *PYCRL* in patients with KIRP was positively correlated with CD4+ T-cell infiltration (Cor = 0.187, $p = 2.50 \times 10^{-3}$; Fig. 9C).

4. Discussion

PYCR has been reported to be overexpressed in various types of tumors, such as bladder, prostate, and gastric cancers [14]. However, PYCR expression has not yet been reported in patients with KIRP. Initially, we compared the expression levels of PYCR in patients with KIRP according to sample types, sex, age, and individual cancer stage and found that PYCR transcript levels were considerably upregulated in patients with KIRP. Interestingly, our results showed that *PYCR1* and *PYCR2* transcript levels were markedly upregulated in females than in males, and patients aged 21–40 years had higher *PYCR1* and *PYCR2* transcript levels than patients in other age groups. However, studies have confirmed that the incidence of RCC in males is higher than that in females [15]. Whether *PYCR1* and *PYCR2* differences in expression by sex and age are associated with the onset and prognosis of KIRP has not yet been reported. In addition, the number of cases in some individual groups was small. Hence, this requires further investigation. Furthermore, we found an extensive positive correlation between *PYCR1*, *PYCR2*, and the pathological stage of patients with KIRP. Our results also showed that *PYCR1*, *PYCR2*, and *PYCRL* were altered by 4%, 7%, and 6%, respectively, in 280 patients with KIRP. We also found that *PYCR1* and *PYCRL* promoter methylation levels were considerably downregulated in patients with KIRP. Genetic changes and promoter methylation often result in abnormal gene expression and function. Increased expression of *PYCR1* and *PYCRL* caused by genetic changes and promoter methylation may also serve as an important factor in KIRP progresion. In addition, we found that the methylation levels of CpG sites in PYCR (*PYCR1*: cg25759517 and cg19202384; *PYCR2*: cg07049680, cg23091741, and cg06086141; *PYCRL*: cg26507094) were notably correlated with the prognosis of patients with KIRP. This revealed that the methyla-

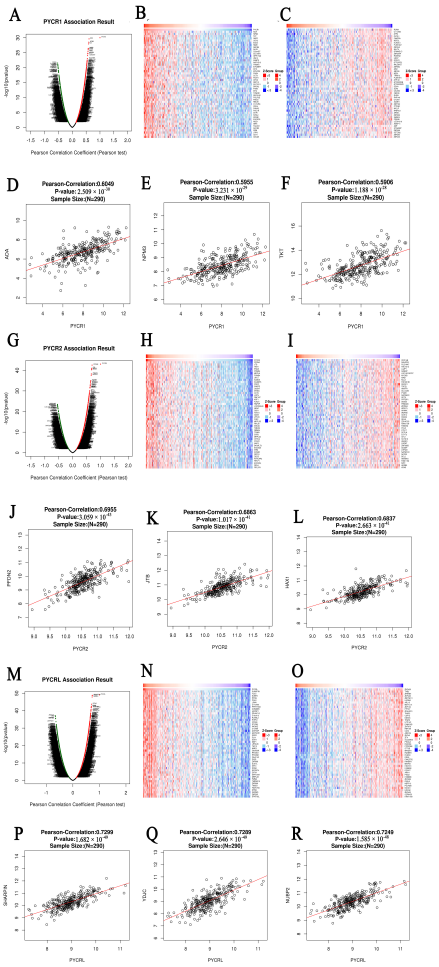

Fig. 8. Genes differentially expressed in correlation with PYCR expression in KIRP (LinkedOmics). (A) Pearson test was used to analyze correlations between *PYCR1* expression and genes differentially expressed in patients with KIRP. (B,C) Heatmaps showing genes positively and negatively correlated, respectively, with *PYCR1* in patients with KIRP (top 50 genes). (D,E,F) The scatter plots show Pearson's correlation of *PYCR1* expression with expression of *ADA*, *NPM*, and *TKT,* respectively, in patients with KIRP. (G) Pearson test was used to analyze correlations between *PYCR2* expression and genes differentially expressed in patients with KIRP. (H,I) Heatmaps showing genes positively and negatively correlated, respectively, with *PYCR2* in patients with KIRP (top 50 genes). (J,K,L) The scatter plots show Pearson's correlation of *PYCR2* expression with expression of *PFDN2*, *JTB*, and *HAX1*, respectively, in patients with KIRP. (M) Pearson test was used to analyze correlations between *PYCRL* expression and genes differentially expressed in patients with KIRP. (N,O) Heatmaps showing genes positively and negatively correlated, respectively, with *PYCRL* in patients with KIRP (top 50 genes). (P,Q,R) The scatter plots show Pearson's correlation of *PYCRL* expression with expression of *SHARPIN*, *YDJC*, and *NUBP2*, respectively, in patients with KIRP.

tion levels of PYCR act as effective prognostic biomarkers for KIRP, indicating that PYCR may play a critical role in KIRP progression. The most frequently altered neighboring genes of PYCR for *PYCR1* were (*ALYREF*, *ANAPC11*, and *ARHGDIA*), *PYCR2* were (*PBRM1*, *CDKN2A*, and *ALK*), and *PYCRL* were (*MT-CO2*, *BLK*, and *C2CD5*). In cancer patients with high *PYCR1* expression, increased *PYCR1* activity is associated with higher expression of oncogenes, such as *ALYREF*, *ANAPC11*, and *ARHGDIA*. *PYCR1*-driven oncogenes promote tumor cell proliferation and metastasis [16–18]. *PBRM1*, *CDKN2A*, and *ALK* are frequently mutated in lung cancer and are associated with tumor resistance [19]. *MT-CO2* is a mitochondrial gene whose mutation has been widely reported in various human tumors. *MT-CO2* variation may be a potential prognostic biomarker in *MUTYH*-associated polyposis patients [20]. *CDKN2A* is the second most common tumor suppressor gene in cancers. *CDKN2A* is frequently altered in chordoma [21]. In conclusion, these gene alterations may be involved in the occurrence and development of KIRP to different degrees and in different pathways. Finally, we assessed the prognostic value of PYCR expression in patients with KIRP. Our results showed that patients with KIRP with low *PYCR1* and *PYCR2* expression had longer survival rates than those with high *PYCR1* and *PYCR2* expression. Thus, *PYCR1* and *PYCR2* may serve as potential prognostic markers in patients with KIRP.

We further evaluated the potential interactions between PYCR and its neighboring genes. We found that PYCR and its neighboring genes are linked to a complex interaction network through co-expression, physical interactions, and prediction. Next, we evaluated the functions of PYCR and its neighboring genes. We found that the molecular functions of *PYCR1* and its neighboring genes were tumor-associated voltage-gated calcium channel activity, phospholipid binding, and ubiquitin-like protein ligase binding. For instance, the voltage-gated calcium channel is closely related to cancer pain and inhibiting its activity can reduce cancer pain [22]. In addition, inhibition of T-type voltage-gated calcium channels showed antiproliferative and cytotoxic effects and is an important anticancer target [23]. Neuronally expressed developmentally downregulated 4 (NEDD4) is a ubiquitin-like protein ligase that accelerates tumor growth and metastasis by regulating the microRNA-132/NRF2 axis [24]. NEDD4 is a potential therapeutic target for the prevention of tumor recurrence and metastasis. In addition, we found that nuclear receptor binding, DNA-binding transcription activator activity, and RNA polymerase II-specificity, which are related to tumorigenesis and development, were the molecular functions of *PYCR2* and its neighboring genes. For example, overexpression of nuclear receptor-binding protein 1 inhibits colorectal cancer cell proliferation and promotes apoptosis [25]. The KEGG pathway of *PYCR2* and its neighboring genes is involved in cancer pathways. In

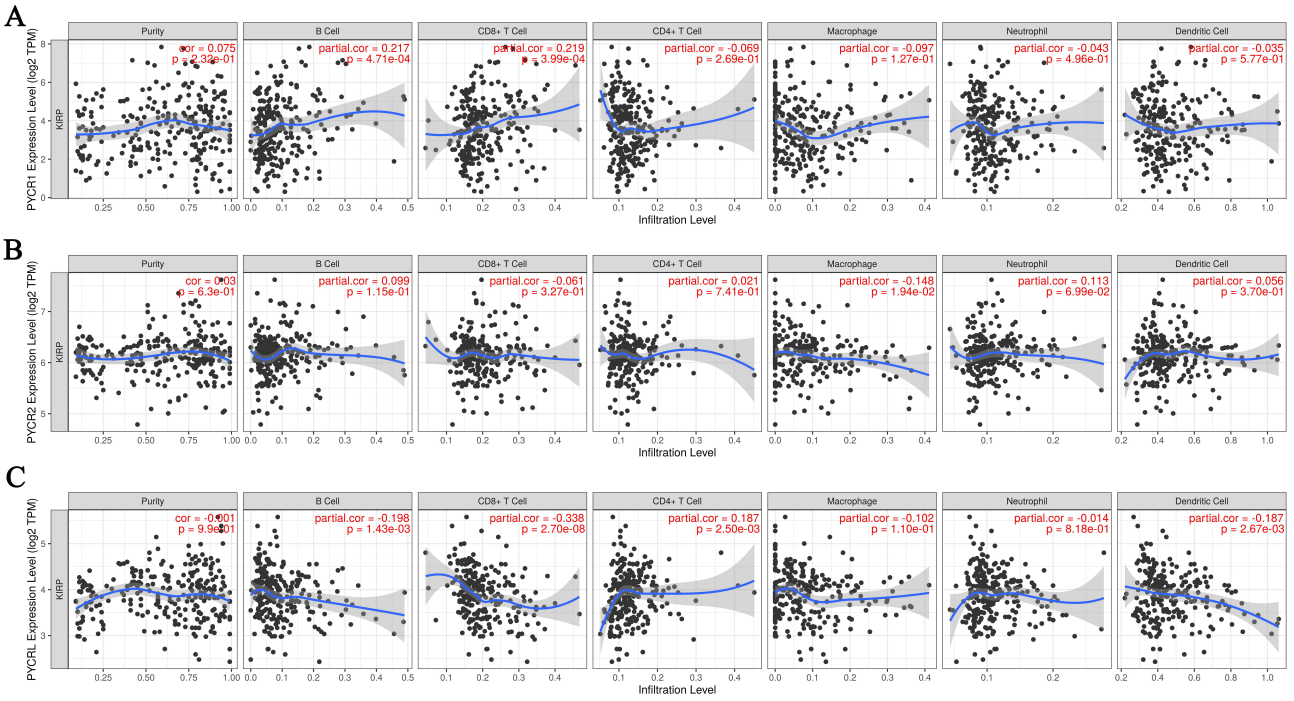

Fig. 9. The correlation between PYCR and immune cell infiltration in KIRP (TIMER). (A) *PYCR1*. (B) *PYCR2*. (C) *PYCRL*.

addition, the molecular functions associated with *PYCRL* and its neighboring genes mainly include oxidoreductase, kinase, and GTPase-regulatory activities related to tumor metabolism. Their KEGG pathway analysis revealed their involvment in proline metabolism. Proline has been shown to act as a potent anti-oxidative stress agent capable of protecting cells from various reactive oxygen species (ROS) inducers. Excessive ROS production is detrimental, through oxidative damage to DNA, proteins, and lipids, to the survival of cancer cells. In summary, regulating the functions of PYCR and its neighboring genes may be an important strategy for the treatment of KIRP.

The increasing incidence of various cancers constitutes an urgent need to identify accurate early diagnostic markers and develop more effective treatments. MicroRNAs (miRNAs) are small non-coding RNAs with great potential as diagnostic markers and therapeutic targets in cancer clinics. Therefore, we explored miRNA targets of PYCR in patients with KIRP. We found that miR-21, miR-221, miR-222, miR-410, miR-202, and miR-508 are targets of *PYCR1*. In recent years, many studies have shown that targeting miR-21 in combination with conventional chemotherapy drugs can improve therapeutic outcomes and overcome drug resistance and tumor recurrence [26,27]. Inhibition of miR-221-3-p and miR-222-3-p can prevent cancer cell viability, migration, and invasion and promote apoptosis [28]. miR-221/222 has potential as an auxiliary diagnostic marker for tumors [29]. miR-410 acts as a cancer inducer in colorectal cancer, and miR-410-3-p promotes colorectal cancer cell migration and invasion by activating the NF-κB pathway [30]. miR-202 inhibits the proliferation, invasion, and migration of breast cancer cells by targeting the *ROCK1* gene. Downregulation of miR-202 is positively associated with poor prognosis in breast cancer patients [31]. miR-508-3p considerably inhibited the epithelial-mesenchymal transition in triple-negative breast cancer cells by regulating *ZEB1* expression. Thus, miR-508-3p may serve as a potential therapeutic target for triple-negative breast cancer [32]. Besides, our results showed that the miRNA targets of *PYCR2* in patients with KIRP were miR-148A, miR-152, miR-148B, miR-153, miR-23A, miR-23B, miR-221, miR-222, miR-15A, miR-16, miR-15B, miR-195, miR-424, and miR-497. The expression of mutated miRNA-148/152 family members (miR-148A, miR-148B, and miR-152) contributes to human carcinogenesis. Hence, they may serve as useful biomarkers for the early diagnosis and tumor development in non-small cell lung cancer (NSCLC) patients [33]. miR-23A/B promotes tumor growth and inhibits apoptosis by targeting programmed cell death 4 (PDCD4) in gastric cancer [34]. The miR-15/16/195/424/497 family plays an important role in the occurrence, progression, and treatment resistance of colorectal cancer [35]. Furthermore, miR-135A, miR-135B, miR-204, miR-211, miR-383, miR-93, miR-302A, miR-302B, miR-302C, miR-302D, miR-372, miR-373, miR-520E, miR-520A, miR-526B, miR-520B, miR-520C, miR-520D, miR-199A, and miR-199B comprised the miRNA targets of *PYCRL* in patients with KIRP. Studies have confirmed that miR-135A-5p and miR-135B-5p can inhibit the proliferation, migration, invasion, and

apoptosis of colorectal cancer cells [36]. miR-211 and miR-204 reduce gastric cancer cell proliferation, metastasis, and activation of protein kinase B (PKB/AKT) [37]. Overexpression of miR-383 inhibits gastric cancer cell proliferation and promotes apoptosis [38]. miR-302A/B/C/D synergistically repressed breast cancer resistance protein (BCRP) expression and increased drug sensitivity in breast cancer cells. As such, it may be a potential target for reversing BCRP-mediated chemoresistance in breast cancer [39]. In summary, the miRNA targets of PYCR are associated with tumor cell proliferation, migration, invasion, and drug resistance and may serve as promising targets for cancer therapy. However, their relationship with KIRP has not been fully elucidated. These results suggest that miRNAs of PYCR may act as potential therapeutic targets for treating KIRP.

We explored the correlation between differentially expressed genes and PYCR expression in patients with KIRP. We found that the expression of 20,023 genes was correlated with *PYCR1* expression. *ADA*, *NPM3*, and *TKT* were the top three genes positively correlated with the expression of *PYCR1*. Adenosine deaminase (ADA) regulates intracellular and extracellular adenosine concentrations by converting adenosine to inosine. Adenosine accumulates in high concentrations in tumors and exerts a series of malignancy-promoting effects [40]. Transketolase (TKT) is a key enzyme in the non-oxidative pentose phosphate pathway. TKT can promote the development of liver cancer in a non-metabolic manner through its nuclear localization and EGFR pathway [41]. In addition, we found that *PFDN2*, *JTB*, and *HAX1* were the top three genes positively correlated with the expression of *PYCR2*. Prefoldin subunits (PFDN2) are involved in cancer progression. PFDN2 may serve as poor prognostic markers for gastric cancer [42]. *JTB* is a tumor suppressor gene in various malignancies and can be used as a biomarker for breast cancer [43]. Studies have confirmed that HS-1-associated protein-1 (HAX1) enhances non-small cell lung cancer survival and metastasis through the AKT/mammalian target of the rapamycin (MTOR) and double minute 2 protein (MDM2)/P53 signaling pathways [44]. Furthermore, *SHARPIN*, *YDJC*, and *NUBP2* were the top three genes positively correlated with the expression of *PYCRL*. SHARPIN plays an important role in tumorigenesis. Overexpression of SHARPIN promotes tumor progression in ovarian cancer [45]. Chitooligosaccharide deacetylase homolog (YDJC) contributes to induction of protein phosphatase 2A (PP2A) ubiquitination by increasing epithelial-mesenchymal transition (EMT). Hence, *YDJC* may become a new target for antitumor therapy [46]. Therefore, targeting these genes may provide adjuvant therapy for KIRP.

Immunotherapy is a novel clinical cancer treatment. Tumor immune infiltration is closely related to clinical prognosis. As expected, the expression level of PYCR in patients with KIRP was positively or negatively correlated with the level of immune cell infiltration. B-cell-mediated inflammation may play an important role in promoting the progression of aggressive malignancies. However, data from preclinical studies have shown significant differences in the role of B cells at different stages of cancer development. In mouse models of precancerous lesions, B cells appear to cause inflammation, which in turn induces precancerous lesions [47]. CD8+ T cells play a central role in antitumor immunity. CD8+ T cells are activated upon stimulation by tumor antigens and then differentiate into functional cells and migrate to the tumor site. Activated CD8+ T cells can directly destroy tumor cells by releasing perforin and granzymes and by inducing death ligand/death receptor-mediated apoptosis. They also secrete cytokines to regulate the immune system in tumor cells. However, disturbances in mitochondrial dynamics can affect CD8+ T cell function. Overall, mitochondrial abnormalities in CD8+ T cells contribute to cancer development [48]. Therefore, targeting PYCR or PYCR-related regulatory targets may be a feasible strategy for regulating immune cell infiltration in patients with KIRP.

5. Conclusions

This study systematically analyzed the expression, gene regulatory network, prognostic value, and target prediction of *PYCR* in patients with KIRP, elucidated the relationship between *PYCR* and KIRP, and provided new insights into KIRP treatment.

Abbreviations

PYCR, Pyrroline-5-carboxylate reductase; KIRP, kidney renal papillary cell carcinoma; KEGG, Kyoto Encyclopedia of Genes and Genome; GO, Gene Ontology; RCC, renal cell carcinoma; PPI, protein-protein interactions; GEPIA, Gene Expression Profiling; miRNA, MicroRNA.

Availability of Data and Materials

The datasets used and/or analyzed during the current study are available from the corresponding author on reasonable request.

Author Contributions

JC and YS performed data analysis work and aided in writing the manuscript. ZS designed the study and assisted in writing the manuscript. LL, YC, LD, QX, QL, XL, and JZ edited the manuscript. All authors read and approved the final manuscript.

Ethics Approval and Consent to Participate

Not applicable.

Acknowledgment

We appreciate the funding support from the Guangdong Medical University, Zhanjiang, and Guangdong province.

Funding

This research was funded by Guangdong province ordinary colleges and universities young innovative talents project (4SG21202G), national pharmaceutical economic information network science and technology communication innovation project of chinese pharmaceutical association (CMEI2021KPYJ00310), postdoctoral Foundation of Guangdong Medical University (4SG22292G), and the project of financial fund science and technology special competitive allocation of Zhanjiang (Zhanke[2010]174).

Conflict of Interest

The authors declare no conflict of interest.

References

[1] Xia C, Dong X, Li H, Cao M, Sun D, He S, *et al*. Cancer statistics in China and United States, 2022: profiles, trends, and determinants. Chinese Medical Journal. 2022; 135: 584–590.

[2] Bray F, Ferlay J, Soerjomataram I, Siegel RL, Torre LA, Jemal A. Global cancer statistics 2018: GLOBOCAN estimates of incidence and mortality worldwide for 36 cancers in 185 countries. CA - A Cancer Journal for Clinicians. 2018; 68: 394–424.

[3] Znaor A, Lortet-Tieulent J, Laversanne M, Jemal A, Bray F. International variations and trends in renal cell carcinoma incidence and mortality. European Urology. 2015; 67: 519–530.

[4] Courthod G, Tucci M, Di Maio M, Scagliotti GV. Papillary renal cell carcinoma: A review of the current therapeutic landscape. Critical Reviews in Oncology/Hematology. 2015; 96: 100–112.

[5] Sun J, Tang Q, Gao Y, Zhang W, Zhao Z, Yang F, *et al*. VHL mutation-mediated SALL4 overexpression promotes tumorigenesis and vascularization of clear cell renal cell carcinoma via Akt/GSK-3β signaling. Journal of Experimental & Clinical Cancer Research. 2020; 39: 104.

[6] Li Y, Bie J, Song C, Liu M, Luo J. PYCR, a key enzyme in proline metabolism, functions in tumorigenesis. Amino Acids. 2021; 53: 1841–1850.

[7] Ding Z, Ericksen RE, Escande-Beillard N, Lee QY, Loh A, Denil S, *et al*. Metabolic pathway analyses identify proline biosynthesis pathway as a promoter of liver tumorigenesis. Journal of Hepatology. 2020; 72: 725–735.

[8] Cai F, Miao Y, Liu C, Wu T, Shen S, Su X, *et al*. Pyrroline-5-carboxylate reductase 1 promotes proliferation and inhibits apoptosis in non-small cell lung cancer. Oncology Letters. 2018; 15: 731–740.

[9] Sahu N, Dela Cruz D, Gao M, Sandoval W, Haverty P, Liu J, *et al*. Proline Starvation Induces Unresolved ER Stress and Hinders mTORC1-Dependent Tumorigenesis. Cell Metabolism. 2016; 24: 753–761.

[10] Zeng T, Zhu L, Liao M, Zhuo W, Yang S, Wu W, *et al*. Knockdown of PYCR1 inhibits cell proliferation and colony formation via cell cycle arrest and apoptosis in prostate cancer. Medical Oncology. 2017; 34: 27.

[11] Dang HH, Ta HDK, Nguyen TTT, Anuraga G, Wang CY, Lee KH, *et al*. Identifying GPSM family members as potential biomarkers in breast cancer: A comprehensive bioinformatics analysis. Biomedicines. 2021; 9: 1144.

[12] Dang HH, Ta HDK, Nguyen TTT, Anuraga G, Wang CY, Lee KH, *et al*. Prospective role and immunotherapeutic targets of sideroflexin protein family in lung adenocarcinoma: evidence from bioinformatics validation. Functional & Integrative Genomics. 2022; 22: 1057–1072.

[13] Situ Y, Xu Q, Deng L, Zhu Y, Gao R, Lei L, *et al*. System analysis of VEGFA in renal cell carcinoma: The expression, prognosis, gene regulation network and regulation targets. International Journal of Biological Markers. 2022; 37: 90–101.

[14] Xiao S, Yao X, Ye J, Tian X, Yin Z, Zhou L. Epigenetic modification facilitates proline synthase PYCR1 aberrant expression in gastric cancer. Biochimica et Biophysica Acta - Gene Regulatory Mechanisms. 2022; 1865: 194829.

[15] Bahadoram S, Davoodi M, Hassanzadeh S, Bahadoram M, Barahman M, Mafakher L. Renal cell carcinoma: an overview of the epidemiology, diagnosis, and treatment. Giornale Italiano di Nefrologia. 2022; 39: 2022-vol3.

[16] Wang JZ, Zhu W, Han J, Yang X, Zhou R, Lu HC, *et al*. The role of the HIF-1α/ALYREF/PKM2 axis in glycolysis and tumorigenesis of bladder cancer. Cancer Communications. 2021; 41: 560–575.

[17] Zhang Y, Zhou H. LncRNA BCAR4 promotes liver cancer progression by upregulating ANAPC11 expression through sponging miR-1261. International Journal of Molecular Medicine. 2020; 46: 159–166.

[18] Zhou KY, Zhou YH, Ji HL, Luo YK. MiR-497 promotes the migration and invasion of human medulloblast Daoy cell line through targeted regulation of ARHGDIA in vitro. Neuroscience Letters. 2022; 772: 136469.

[19] Shang Y, Li X, Liu W, Shi X, Yuan S, Huo R, *et al*. Comprehensive genomic profile of Chinese lung cancer patients and mutation characteristics of individuals resistant to icotinib/gefitinib. Scientific Reports. 2020; 10: 20243.

[20] Errichiello E, Balsamo A, Cerni M, Venesio T. Mitochondrial variants in MT-CO2 and D-loop instability are involved in MUTYH-associated polyposis. Journal of Molecular Medicine. 2015; 93: 1271–1281.

[21] Cottone L, Eden N, Usher I, Lombard P, Ye H, Ligammari L, *et al*. Frequent alterations in p16/CDKN2A identified by immunohistochemistry and FISH in chordoma. The Journal of Pathology: Clinical Research. 2020; 6: 113–123.

[22] Trevisan G, Oliveira SM. Animal Venom Peptides Cause Antinociceptive Effects by Voltage-gated Calcium Channels Activity Blockage. Current Neuropharmacology. 2022; 20: 1579–1599.

[23] Bhargava A, Saha S. T-Type voltage gated calcium channels: a target in breast cancer? Breast Cancer Research and Treatment. 2019; 173: 11–21.

[24] Mao M, Yang L, Hu J, Liu B, Zhang X, Liu Y, *et al*. Oncogenic E3 ubiquitin ligase NEDD4 binds to KLF8 and regulates the microRNA-132/NRF2 axis in bladder cancer. Experimental & Molecular Medicine. 2022; 54: 47–60.

[25] Liao Y, Yang Z, Huang J, Chen H, Xiang J, Li S, *et al*. Nuclear receptor binding protein 1 correlates with better prognosis and induces caspase-dependent intrinsic apoptosis through the JNK signalling pathway in colorectal cancer. Cell Death & Disease. 2018; 9: 436.

[26] Arghiani N, Matin MM. MiR-21: a Key Small Molecule with Great Effects in Combination Cancer Therapy. Nucleic Acid Therapeutics. 2021; 31: 271–283.

[27] Liu F, Mao H, Chai S, Mao H. Meta-analysis of the diagnostic value of exosomal miR-21 as a biomarker for the prediction of cancer. Journal of Clinical Laboratory Analysis. 2021; 35: e23956.

[28] Zheng L, Yan B, Jin G, Han W, Wang H, Wang Z, *et al*. Circ_0003159 upregulates LIFR expression through competitively binding to miR-221-3p/miR-222-3p to block gastric can-

cer development. Journal of Molecular Histology. 2022; 53: 173–186.

[29] Cai S, Ma J, Wang Y, Cai Y, Xie L, Chen X, *et al*. Biomarker Value of miR-221 and miR-222 as Potential Substrates in the Differential Diagnosis of Papillary Thyroid Cancer Based on Data Synthesis and Bioinformatics Approach. Frontiers in Endocrinology. 2022; 12: 794490.

[30] Ma ZH, Shi PD, Wan BS. MiR-410-3p activates the NF-κB pathway by targeting ZCCHC10 to promote migration, invasion and EMT of colorectal cancer. Cytokine. 2021; 140: 155433.

[31] Xu F, Li H, Hu C. MiR-202 inhibits cell proliferation, invasion, and migration in breast cancer by targeting ROCK1 gene. Journal of Cellular Biochemistry. 2019; 120: 16008–16018.

[32] Guo SJ, Zeng HX, Huang P, Wang S, Xie CH, Li SJ. MiR-508-3p inhibits cell invasion and epithelial-mesenchymal transition by targeting ZEB1 in triple-negative breast cancer. European Review for Medical and Pharmacological Sciences. 2018; 22: 6379–6385.

[33] Li L, Chen YY, Li SQ, Huang C, Qin YZ. Expression of miR-148/152 family as potential biomarkers in non-small-cell lung cancer. Medical Science Monitor. 2015; 21: 1155–1161.

[34] Hu X, Wang Y, Liang H, Fan Q, Zhu R, Cui J, *et al*. MiR-23a/b promote tumor growth and suppress apoptosis by targeting PDCD4 in gastric cancer. Cell Death & Disease. 2017; 8: e3059.

[35] Guo ST, Jiang CC, Wang GP, Li YP, Wang CY, Guo XY, *et al*. MicroRNA-497 targets insulin-like growth factor 1 receptor and has a tumour suppressive role in human colorectal cancer. Oncogene. 2013; 32: 1910–1920.

[36] Zhang Y, Zhang Z, Yi Y, Wang Y, Fu J. CircNOL10 Acts as a Sponge of miR-135a/b-5p in Suppressing Colorectal Cancer Progression via Regulating KLF9. OncoTargets and Therapy. 2020; 13: 5165–5176.

[37] Shi Y, Chen X, Xi B, Yu X, Ouyang J, Han C, *et al*. SNP rs3202538 in 3'UTR region of ErbB3 regulated by miR-204 and miR-211 promote gastric cancer development in Chinese population. Cancer Cell International. 2017; 17: 81.

[38] Zhu C, Huang Q, Zhu H. MiR-383 Inhibited the Cell Cycle Progression of Gastric Cancer Cells via Targeting Cyclin E2. DNA and Cell Biology. 2019; 38: 849–856.

[39] Wang Y, Zhao L, Xiao Q, Jiang L, He M, Bai X, *et al*. MiR-302a/b/c/d cooperatively inhibit BCRP expression to increase drug sensitivity in breast cancer cells. Gynecologic Oncology. 2016; 141: 592–601.

[40] Battisti V, Maders LDK, Bagatini MD, Battisti IE, Bellé LP, Santos KF, *et al*. Ectonucleotide pyrophosphatase/phosphodiesterase (E-NPP) and adenosine deaminase (ADA) activities in prostate cancer patients: Influence of Gleason score, treatment and bone metastasis. Biomedicine & Pharmacotherapy. 2013; 67: 203–208.

[41] Qin Z, Xiang C, Zhong F, Liu Y, Dong Q, Li K, *et al*. Transketolase (TKT) activity and nuclear localization promote hepatocellular carcinoma in a metabolic and a non-metabolic manner. Journal of Experimental & Clinical Cancer Research. 2019; 38: 154.

[42] Yesseyeva G, Aikemu B, Hong H, Yu C, Dong F, Sun J, *et al*. Prefoldin subunits (PFDN1-6) serve as poor prognostic markers in gastric cancer. Bioscience Reports. 2020; 40: BSR20192712.

[43] Jayathirtha M, Neagu AN, Whitham D, Alwine S, Darie CC. Investigation of the effects of overexpression of jumping translocation breakpoint (JTB) protein in MCF7 cells for potential use as a biomarker in breast cancer. American Journal of Cancer Research. 2022; 12: 1784–1823.

[44] Liang Z, Zhong Y, Meng L, Chen Y, Liu Y, Wu A, *et al*. HAX1 enhances the survival and metastasis of non-small cell lung cancer through the AKT/mTOR and MDM2/p53 signaling pathway. Thoracic Cancer. 2020; 11: 3155–3167.

[45] Wang G, Zhuang Z, Cheng J, Yang F, Zhu D, Jiang Z, *et al*. Overexpression of SHARPIN promotes tumor progression in ovarian cancer. Experimental and Molecular Pathology. 2022. (online ahead of print)

[46] Kim EJ, Park MK, Kang GJ, Byun HJ, Kim HJ, Yu L, *et al*. YDJC Induces Epithelial-Mesenchymal Transition via Escaping from Interaction with CDC16 through Ubiquitination of PP2a. Journal of Oncology. 2019; 2019: 3542537.

[47] Patel AJ, Richter A, Drayson MT, Middleton GW. The role of B lymphocytes in the immuno-biology of non-small-cell lung cancer. Cancer Immunology, Immunotherapy. 2020; 69: 325–342.

[48] Zhang L, Zhang W, Li Z, Lin S, Zheng T, Hao B, *et al*. Mitochondria dysfunction in CD8+ T cells as an important contributing factor for cancer development and a potential target for cancer treatment: a review. Journal of Experimental and Clinical Cancer Research. 2022; 41: 227.